

# PI Controller Design for DC Motor Using Different Power Electronic Converters

Khalil Azha Mohd Annuar<sup>1</sup>, Wan Norhisyam Abd Rashid<sup>1</sup>, Mohd Razali Bin Mohamad Sapiee<sup>1</sup>,

Nik Azran Ab Hadi<sup>1</sup>, Mohd Syahril bin Mohd Azali<sup>2</sup>

<sup>1</sup>Faculty of Electrical Engineering Technology, Universiti Teknikal Malaysia Melaka,  
Hang Tuah Jaya, 75450 Melaka, Malaysia.

<sup>2</sup>DDZ Department, Telekom Malaysia Sdn. Bhd., No. 176 & 177, Jln Dato Bandar Tunggal,  
70000 Seremban, Negeri Sembilan.

*khalilazha@utem.edu.my*

**Abstract**—In this paper, the design of a PI controller of a DC motor closed-loop torque control system is presented. The controllers are designed using small signal models and then verified using large signal simulation. A step by step design procedure is carried out to determine the response of each loop and appropriate parameters of the PI controllers are shown throughout this study assisted by Bode Plot and pole zero map techniques. In this paper also, there is comparison made when using different power electronic converters between 3-phase controlled rectifier and 4-quadrant switch mode DC-DC converter. It is highly demanded to design the PI controllers that will result in high performance in terms of high speed of response, low steady state error and high degree of stability. In this paper, simulation studies are included to show that the PI controllers designed could control the torque as desired and achieve satisfactory performance. The analysis of performance of torque and speed is compared with the desired (reference) values based on MATLAB/SIMULINK simulation.

**Index Terms**—3-Phase Controlled Rectifier; 4-Quadrant Switch-Mode Converter; Bode Diagram; Closed-Loop; Current-Controlled System; DC Drive; Gain; PI Controller; Pole And Zero Map Diagram; Unipolar Switching Scheme.

## I. INTRODUCTION

DC motor drives has been used as the most popular drives for speed and torque control applications [1-4]. In many applications, such as robotics and factory automation these motor needs precise controller [5-6]. The purpose of a motor speed controller is to take a signal representing the demanded torque or speed, and to drive a motor at the reference value. This type value of control system is called Closed Loop Control System for DC Machine [7]. This control model is better than Open Loop, but more complicated, and may not be required for a simple motor design. Motors come in a variety of forms, and the torque controller's motor drive output will be different depending on these forms. The torque controller presented here is designed as a feedback control system that consists of a power electronic converter, a controller and a DC machine as the load [8].

The controller is designed to drive the system response to a desired (reference) values. In a DC drive closed-loop system, the output variables of the system such as torque and speed are sensed and feedback to be compared with the desired values. The computed error between both desired and output variables is amplified to control the power processing unit, to minimize or eliminate this error. To realize these objectives, there are many approaches being used to control the system

stability, transient and steady state responses of the system and also to search for the appropriate parameters for the controller [9-11].

In this paper, only the Bode Plot techniques will be presented as tools for stability analysis and parameters adjustment of a Proportional and Integral (PI) controller to achieve the control purpose of the DC-motor [12-13]. In order to respond the desired input (reference), the output of the system should equals the reference input. So, the controller is designed with the following objective: i) a zero steady state error ii) a good dynamic response (which implies both a fast transient response with a small settling time and very little overshoot). Figure 1 below is a simple block diagram of the torque controller.

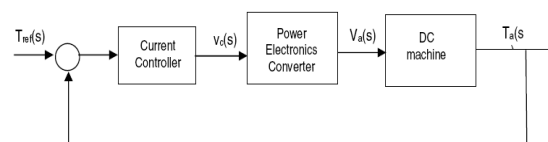


Figure 1: Closed-loop control system for DC drive

## II. 4-QUADRANT SWITCH MODE DC-DC CONVERTER

This converter is composed of two legs in which each leg contains two quadrant converters as in Figure 2.

Assumptions made are that the converters obtained the switching signals from a comparison between control signal  $V_c$  and a triangular waveforms  $V_{tri}$ .

Based on Figure 2, the output voltage  $V_a$ , can vary between  $V_{DC}$  and  $-V_{DC}$ , 0 and  $V_{DC}$  or 0 and  $-V_{DC}$  depending on the type of switching being used either bipolar or unipolar switching type. For discussion, only the bipolar switching type is used as the switching scheme of this converter in this paper. From the switching scheme, we can obtain the switching signal from the comparison between control signal  $V_c$  and the triangular waveform  $V_{tri}$ .

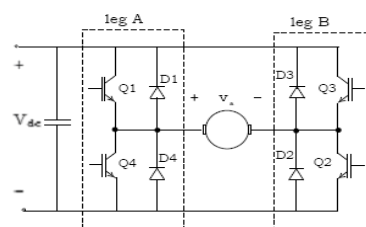


Figure 2: Four quadrant switch mode converter

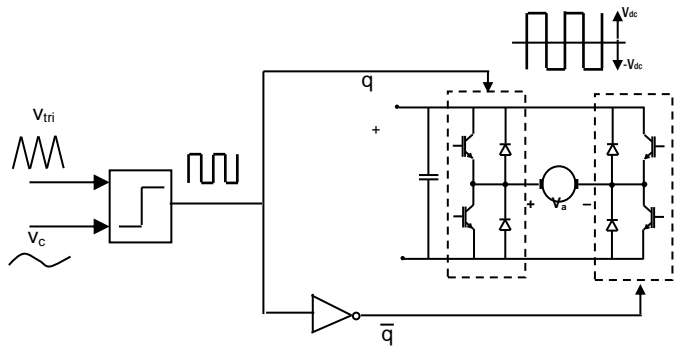


Figure 3: Bipolar switching signal for the switching mode

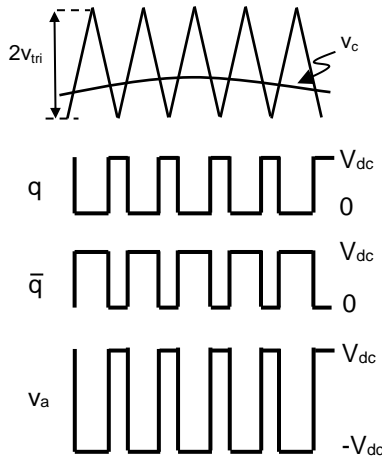


Figure 4: Comparison between the control signal and the triangular waveform

After some derivations, the linear relationship between control signal,  $V_c$ , triangular waveform  $V_{tri}$  and the average voltage can be formulated as Equation (1).

$$V_a(s) = \frac{V_{dc}}{V_{tri}} V_c(s) \quad (1)$$

### III. 3-PHASE CONTROLLED RECTIFIER

This rectifier is the same like a normal 3-phase rectifier but there is a difference in which the diode is being replaced by SCR as shown in Figure 5.

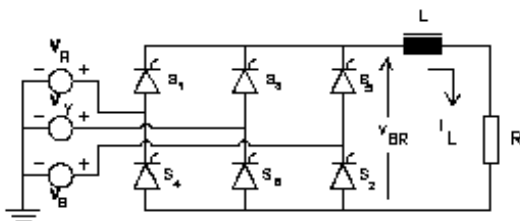


Figure 5: Controlled 3-phase rectifier

The conduction does not begin until the gate signal is applied while SCR is forward bias. As a result, the transition of the output voltage to the maximum instantaneous line-to-line source voltage can be delayed. The delay angle  $\alpha$  is referenced from where the SCR would begin to conduct as if it was a diode. The delay angle is the interval between the SCR becoming forward biased and the gate signal being

applied. The average output voltage as equation (2) and (3).

$$V_o = \left( \frac{3V_{m,L-L}}{\pi} \right) \cos \alpha \quad (2)$$

$$V_o = \frac{3V_{m,L-L}}{\pi} \quad (3)$$

### IV. PROPORTIONAL INTEGRAL (PI) CONTROLLER

In control engineering, a PI Controller (proportional-integral controller) is a feedback controller which drives the plant to be controlled with a weighted sum of the error (difference between the output and desired set-point) and the integral of that value. Figure 6 shown the basic block diagram PI controller. It is a special case of the common PID controller in which the derivative (D) of the error is not used.

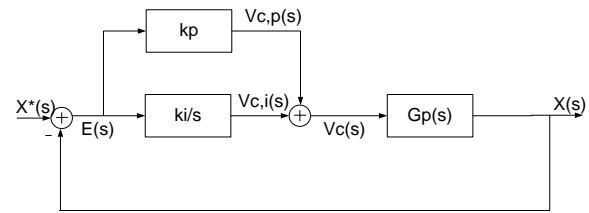


Figure 6: PI controller

The controller output is given by:

$$k_p \Delta + k_i \int \Delta dt \quad (4)$$

where  $\Delta$  is the set-point error.

These proportional integral (PI) controllers will cause the steady state error of the system to be set to zero. The proportional controller produces an output proportional to the error input with,

$$V_{c,p}(s) = k_p E(s) \quad (5)$$

where  $k_p$  is the proportional-controller gain. In torque loops applications, the proportional-controllers alone will result in a steady state error in response to step-change in the input reference. Therefore, normally this controller is combined with the integral controller which described below.

In Figure 6 the output of the integral-controllers can be expressed as:

$$V_{c,i}(s) = \frac{k_i}{s} E(s) \quad (6)$$

where  $k_i$  is the integral gain. This controller responds slowly by virtue of its action is proportional to the time integral of the error. As a result, the steady-state error goes to zeros for a step-change in input because the integrator action continues for as long as the error is not zero.

As shown in Figure 6, the output of both of the controllers can be related by  $V_c(s) = V_{c,p}(s) + V_{c,i}(s)$ . Therefore, using Eqs (5) and Eqs (6), the transfer function of a PI controller is,

$$\frac{V_c(s)}{E(s)} = \left( k_p + \frac{k_i}{s} \right) = \frac{k_i}{s} \left( 1 + \frac{s}{k_i/k_p} \right) \quad (7)$$

V. SMALL SIGNAL MODEL

The parameter for the DC motors are given as follows;

- Ra = 0.8 Ω
- La = 103mH
- KE = Kt = 0.764 Vs/rad
- J = 2kg-m<sup>2</sup>
- Viscous friction constant , B = 0.06 Nm-s
- Rated armature voltage = 120V
- Nrated = 1313rpm

From the Figure 7, this control model is the torque control of DC motor. This model is called a small signal model which is used to find the adjustment value for Kp and Ki from the Bode Plot. The input of this DC motor model is Va, average voltage and the output is T, the DC motor torque.

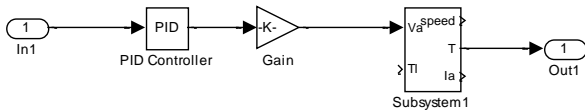


Figure 7: Small Signal Model

A. References 3-Phase Controlled Rectifier

By looking at Figure 8, the zero is situated at the right side of the pole at 0.415. The system will become stable, if the position of the zero is between two poles.

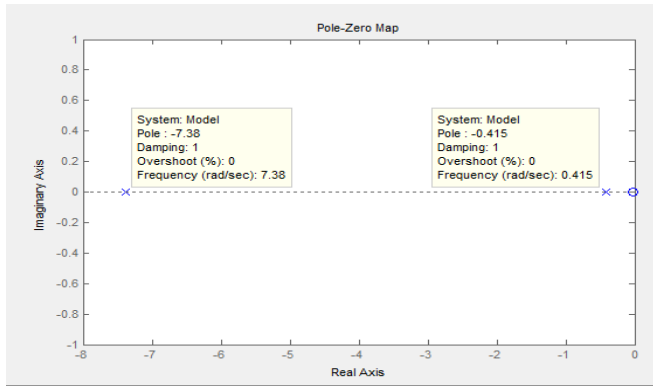


Figure 8: Pole zero map

The value w can be calculated first by finding the difference between the frequencies of both poles which is 7.38-0.415 = 6.965Hz. Then, we can get w from the formula below:

$$w = (6.965) \frac{200}{311} \quad (8)$$

Then by assuming Ki = 1,

$$w = \frac{K_i}{K_p} \quad (9)$$

where  $K_p = \frac{1}{4.48} = 0.2232$

These values will be assigned to the PI controller and the Bode Plot of the system will give the green curve as in Figure 9 next page. The magnitude of the system at frequency 30 Hz will be observed. The objective now is to make the gain 0dB at 30 Hz. From the Bode Plot, the magnitude is 4.41dB. So the system need to be adjusted which is to shift down the Bode Plot -4.41dB.

$$-4.41 = 20 \log K_i \quad (10)$$

where Ki = 0.602.

After getting the value of Ki, the value of Kp can be calculated using Equation (9)

$$K_p = \frac{0.602}{4.48} = 0.1344$$

This value will be assigned to the PI controller in large signal model. Then the magnitude of the new Bode Plot at 30 Hz is 0dB (red curve on Figure 9).

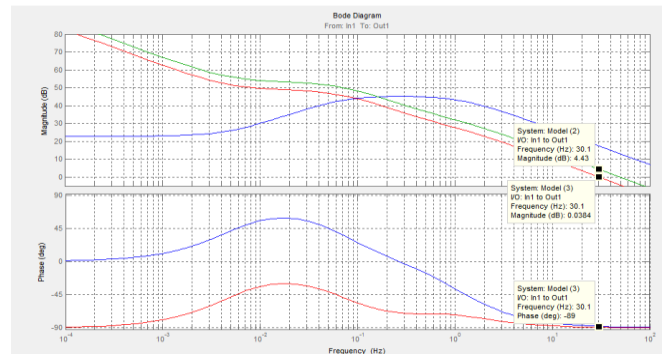


Figure 9: Bode Plot when making small signal using 3-phase controlled rectifier

B. 4-quadrant switch-mode DC-DC converter

The calculations of the all values are the same as the 3-phase controlled rectifier except for when finding the magnitude in Bode Plot during the specified frequency. For the 4-quadrant switch mode DC-DC converter, the frequency is 500 Hz (as it is mentioned that the specifications require the bandwidth:

$$Bandwidth = (Sampling Freq) \frac{1}{10}$$

The system sampling frequency is 5000Hz so the bandwidth is 500Hz. The magnitude value at 500 Hz is -43.1 dB. So the Bode Plot needs to be shifted up 43.1dB (refer to green curve on the Bode Plot of Figure 10)

$$20 \log K_i = 43.1 \quad (11)$$

where Ki = 143.

Using the Equation (9), the value of Kp can be determined as:

$$K_p = \frac{143}{4.48} = 31.92$$

The value of the magnitude at 500 Hz after the adjustment is 0dB (red curve on the Bode Plot of Figure 10). The value of Kp and Ki will be assigned to the PID controller in the large signal model.

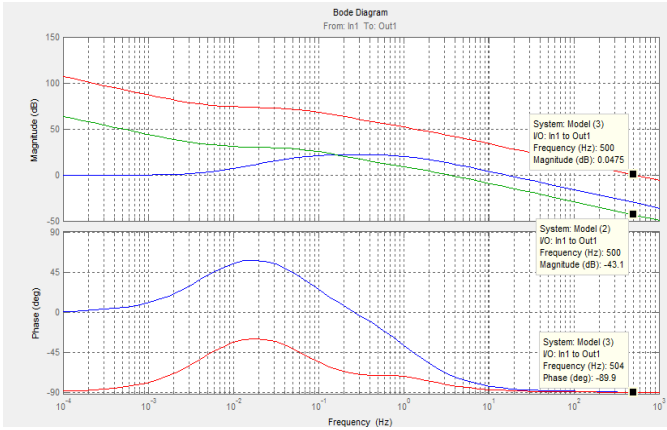


Figure 10: Bode Plot when making small signal analysis using 4-quadrant DC-DC Converter

VI. LARGE SIGNAL SIMULATIONS AND RESULTS

A. 3-Phase Controlled Rectifier

The values  $K_i=0.602$  and  $K_p=0.1344$  are then assigned to the PI controller on large signal model of Figure 11.

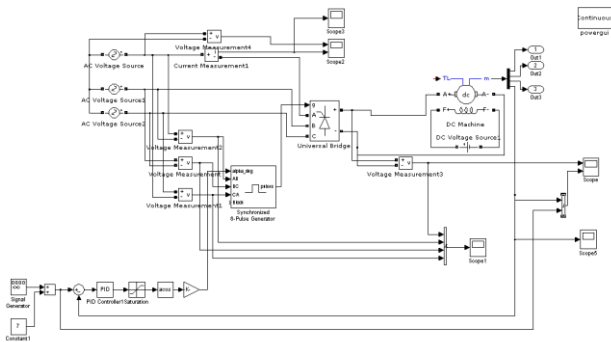


Figure 11: The closed loop signal of the 3-phase controlled rectifier

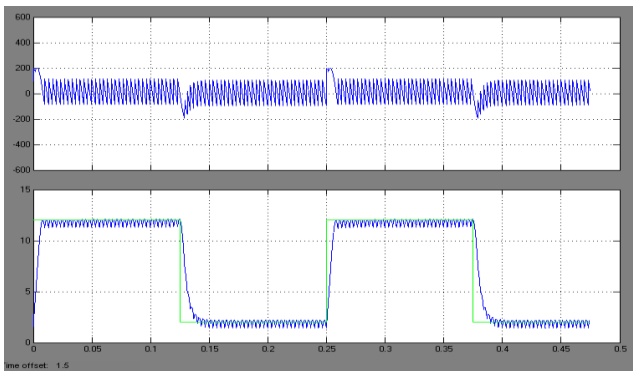


Figure 12: Graph for the signal of the  $T_a$ , output torque when compare to reference torque  $T_{ref}$ . Graph at the top side is the voltage across firing circuit of the SCR bridge rectifier

The top side of the graph in Figure 12 is voltage across the SCR firing circuit (universal bridge) which is required to change the value of the output torque,  $T_a$  (blue signal). The value of the output torque,  $T_a$  will be compared with the  $T_{ref}$  (represented by green signal).

B. 4-quadrant switch-mode DC-DC converter

The values  $K_i=143$  and  $K_p=31.92$  is then applied to the PI controller on large signal model as in Figure 13.

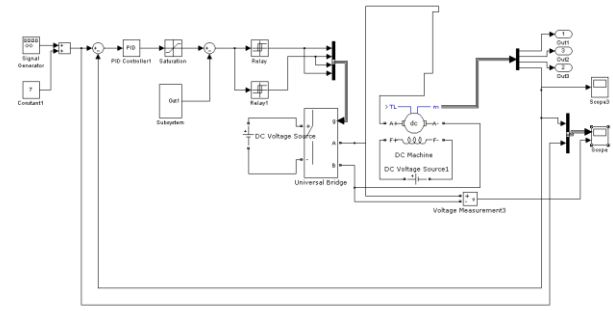


Figure 13: Large signal closed loop model using 4-quadrant switch mode DC-DC converter

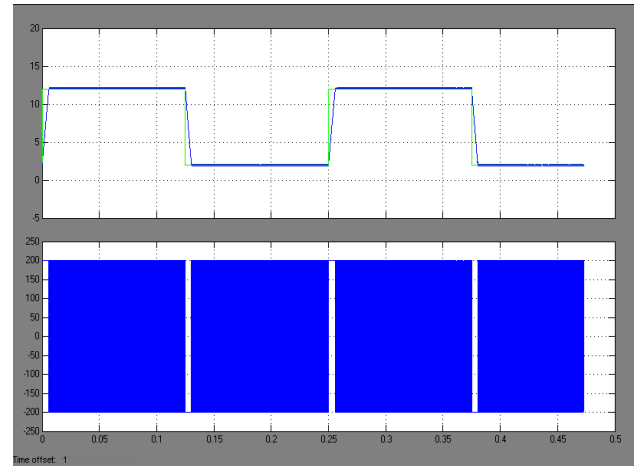


Figure 14: Output Torque For The 4 Quadrant DC-DC Converter

The low side is the voltage on the universal bridge being produced on each 4-quadrant and still the  $T_a$  (represented by blue signal) will change according to the switch of each quadrant. This output torque,  $T_a$  will be compared to the  $T_{ref}$  (represented by the green signal). It can be seen that this system is a bipolar 4-quadrant switch mode DC-DC converter which due to its switching mode, the average voltage  $V_a$ , swings from the value  $-200$  to  $200V$  ( $-V_{dc}$  to  $V_{dc}$ ).

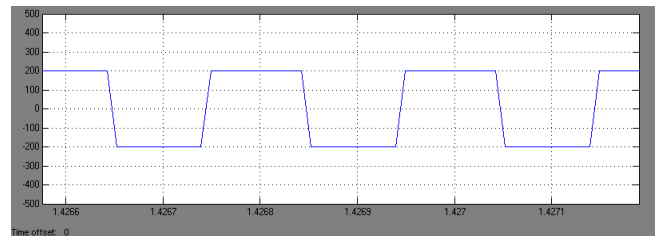


Figure 15: The average voltage,  $V_a$ , as the result of the comparison between  $V_{tri}$  and  $V_c$ .

VII. PERFORMANCE COMPARISON

Comparing Figure 16 of 3-phase controlled rectifier and Figure 18 of 4-quadrant switch-mode DC-DC converter, it shows that the ripple is less when using the 4-quadrant DC-DC converter.

It is observed that the bipolar 4-quadrant scheme gives much lesser ripple in its output current as compared to 3-phase controlled rectifier scheme. This has been proven through the simulations done. The maximum current ripple is reduced by about five times compared to the current ripple in 3-phase controlled rectifier scheme.

As discussed earlier that it is desirable to have a low ripple current in electrical drives which makes the 4-quadrant DC-DC converter switching scheme is preferable.

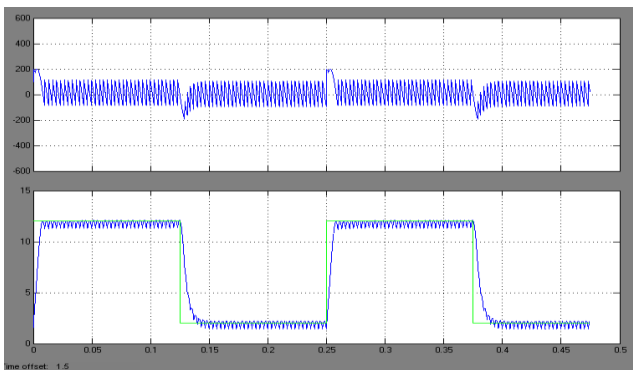


Figure 16: The ripple in the output signal of a 3-phase controlled rectifier

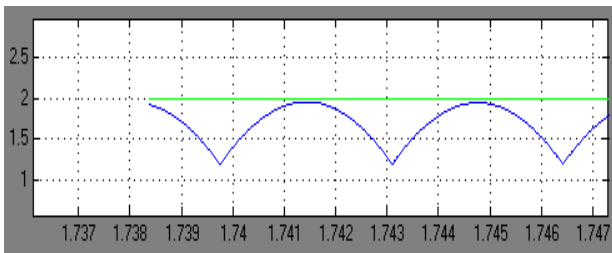


Figure 17: The ripple when zooming. The ripple's value is  $2 - 1.2 = 0.8$

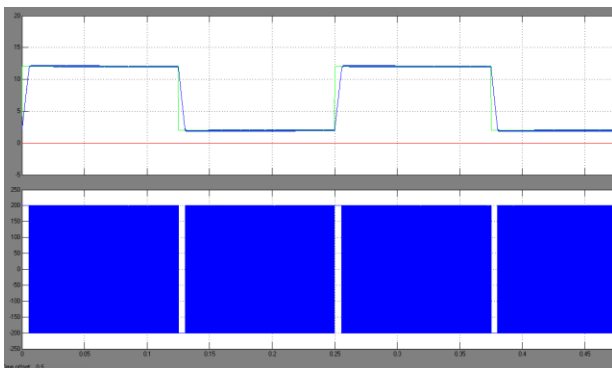


Figure 18: The ripple in the output signal of a 4-quadrant switch-mode DC-DC converter

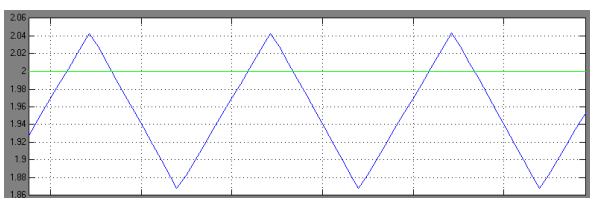


Figure 19: The ripple when zooming. The ripple's value  $2.04 - 1.868 = 0.172$

### VIII. CONCLUSION

Understanding the DC drives involves controlling electric motors in the steady state and in dynamic operations. The control of DC drives can be done with a simple controller such as PI controller. However, in order to design the PI

controller, one needs to understand the open loop control adjustment with Bode Plot and small signal model in MATLAB (SIMULINK). As a conclusion, 4-quadrant switch mode DC-DC converter's (bipolar) performance is better than the rectifier controlled converter in term of ripple and time lag.

### ACKNOWLEDGMENT

The authors would like to thanks for the support given to this research by Ministry of Higher Education Malaysia and Universiti Teknikal Malaysia Melaka (UTeM) for support this paper. Also acknowledge to their gratitude to Dr. Rumzi for his assistance in the completion of this paper.

### REFERENCES

- [1] Umesh Kumar Bansal and Rakesh Narvey, "Speed Control of DC Motor using Fuzzy PID Controller," *Advance in Electronic and Electric Engineering*, Vol. 3, Number 9, pp. 1209-1220, 2013.
- [2] M. Masmoudi, B. El Badi and A. Masmoudi, "Direct Torque Control of Brushless DC Motor Drives With Improved Reliability," in *IEEE Transactions on Industry Applications*, vol. 50, no. 6, pp. 3744-3753, 2014.
- [3] J. A. Riveros, F. Barrero, E. Levi, M. J. Durán, S. Toral and M. Jones, "Variable-Speed Five-Phase Induction Motor Drive Based on Predictive Torque Control," in *IEEE Transactions on Industrial Electronics*, vol. 60, no. 8, pp. 2957-2968, Aug. 2013.
- [4] R.Saidur, S.Mekhilef, M.B.Ali, A.Safari, H.A.Mohammed, "Applications of Variable Speed Drive (VSD) in Electrical Motors Energy Savings," *Renewable and Sustainable Energy Reviews*, Volume 16, Issue 1 pp. 543-550, 2012.
- [5] Ahmad A Mahfouz, M. K. Mohammed, Farhan A. Salem, "Modeling, Simulation and Dynamics Analysis Issues of Electric Motor, for Mechatronics Applications, Using Different Approaches and Verification by MATLAB/Simulink" *International Journal of Intelligent Systems and Applications*, Hong Kong Vol. 5, Issue 5, pp. 39-57, 2013.
- [6] Ritika Pahuja and Narender Kumar, "Android Mobile Phone Controlled Bluetooth Robot using 8051 Microcontroller" *International Journal of Scientific Engineering and Research (IJSER)*, Volume 2, Issue 7, 2014.
- [7] Neerparaj Rai and Bijay Rai, "Neural Network ased Closed loop Speed Control of DC Motor using Arduino Uno," *International Journal of Engineering Trends and Technology*, Volume 4, Issue 2, pp. 137-140, 2013.
- [8] Hengsi Qin and Jonathan W. Kimball, "Closed-Loop Control of DC-DC Dual-Active-Bridge Converters Driving Single-Phase Inverters," in *IEEE Transactions on Power Electronics*, vol. 29, no. 2, pp. 1006-1017, Feb. 2014.
- [9] J. Yao, Z. Jiao and D. Ma, "Adaptive Robust Control of DC Motors With Extended State Observer," in *IEEE Transactions on Industrial Electronics*, vol. 61, no. 7, pp. 3630-3637, July 2014.
- [10] H.E.A. Ibrahim, F.N. Hassan, Anas O. Shomer, "Optimal PID control of a brushless DC motor using PSO and BF techniques," *Ain Shams Engineering Journal*, Volume 5, Issue 2, pp. 391-398, 2014.
- [11] L. Harnefors, S. E. Saarakkala and M. Hinkkanen, "Speed Control of Electrical Drives Using Classical Control Methods," in *IEEE Transactions on Industry Applications*, vol. 49, no. 2, pp. 889-898, March-April 2013.
- [12] A. Rajasekhar, S. Das and A. Abraham, "Fractional Order PID controller design for speed control of chopper fed DC Motor Drive using Artificial Bee Colony algorithm," *2013 World Congress on Nature and Biologically Inspired Computing*, Fargo, ND, 2013, pp. 259-266, 2013.
- [13] Vinod KR Singh Patel and A.K.Pandey, "Modeling and Performance Analysis of PID Controlled BLDC Motor and Different Schemes of PWM Controlled BLDC Motor," *International Journal of Scientific and Research Publications*, Volume 3, Issue 4, April 2013.